Sensitivity Analysis of Stability Influencing Factors for Inverted T-Type Retaining Wall in an Active Limit State Based on Strength Reduction Method and Orthogonal Experimental Design

Yongqing Zeng, *Member, IAENG,* Jiawen Huang, Qisheng Hu, Ruyi Zang, Weidong Hu, Xiaohong Liu, and Hua Luo

***Abstract*—The inverted T-type retaining wall is widely used in geotechnical slope support engineering, which can prevent slope failures and casualties. Due to the lack of theoretical research, engineers cannot accurately evaluate the effect of the inverted T-type retaining structural components on the stability of slopes under design and construction. The deformation law, failure characteristics and mechanical mechanism of the sliding surface in the backfill, and the stability safety factor of inverted T-type retaining wall in an active limit state are analyzed using the finite element limit analysis software OptumG2. To provide a reference for the design of inverted T-type type retaining wall, the stability of inverted T-type retaining wall is studied by using strength reduction method and orthogonal experimental design; in which eleven influencing factors are considered, including the wall stem height, the bottom plate thickness, the wall heel width, the wall stem entirely vertical width, the wall toe width, the base angle of retaining wall, the soil cohesion, the soil internal friction angle, the soil young's modulus, the soil pisson's ratio and the soil unit weight. The influencing factors affecting the safety factor of inverted T-type retaining wall in descending order are the wall stem height, the soil cohesion, the soil internal friction angle, the wall heel width, the wall toe width, the base angle, the bottom plate thickness, the wall stem width, the soil unit weight, the soil pisson's ratio and the soil young's modulus. The research is significant for studying the stability of inverted T-type retaining wall, which can provide references for the design and construction of inverted T-type retaining wall.**

Manuscript received January 22, 2024; revised September 25, 2024. The study was supported by the Natural Science Foundation of Hunan Province of China (Grant No. 2022JJ40160 and Grant No. 2024JJ7209), the Key Scientific Program of Hunan Education Department, China (Grant No. 20A228, Grant No. 22A0472 and Grant No. 23A0496), and the Innovation Project of Hunan Undergraduate Students (Grant No. S202412658013).

Yongqing Zeng is a lecturer in College of Civil Engineering and Architecture, Hunan Institute of Science and Technology, Yueyang, 414000 China. (corresponding author e-mail: yqzeng@hnist.edu.cn).

Jiawen Huang is a postgraduate student in College of Civil Engineering and Architecture, Hunan Institute of Science and Technology, Yueyang, 414000 China. (e-mail: 1403069421@qq.com).

Qisheng Hu is an undergraduate student in Department of Architecture and Civil Engineering, Hunan Urban Construction College, Xiangtan, 411101 China. (e-mail: 1271237998@qq.com).

Ruyi Zang is an undergraduate student in Nanhu College, Hunan Institute of Science and Technology, Yueyang, 414000 China. (e-mail: 2657878737@qq.com).

Weidong Hu is a professor in College of Civil Engineering and Architecture, Hunan Institute of Science and Technology, Yueyang, 414000 China. (e-mail: 11996498@hnist.edu.cn).

Xiaohong Liu is a professor in College of Civil Engineering and Architecture, Hunan Institute of Science and Technology, Yueyang, 414000 China. (e-mail: 11991491@hnist.edu.cn).

Hua Luo is an associate professor in College of Civil Engineering and Architecture, Hunan Institute of Science and Technology, Yueyang, 414000 China. (e-mail: 12015024@hnist.edu.cn).

***Index Terms*—sensitivity analysis, inverted T-type retaining wall, active limit state, strength reduction method, orthogonal experimental design**

I. Introduction

The inverted T-type retaining wall is widely used to stabilize natural slopes or artificial slopes in civil engineering, hydropower engineering, highway engineering and railway engineering [1-3]. The inverted T-type retaining wall, as a reinforced cantilever retaining wall, the structure can combine retaining wall weight with the filling weight on the bottom plate to jointly resist the lateral thrust of the filling. Due to the advantages of saving stone materials, convenient construction, high horizontal shear strength, and good economic benefits, the inverted T-type retaining wall has been widely used in the lacking stone materials, low foundation-bearing capacity, or earthquake-prone regions [4-6]. An inverted T-type retaining wall design should prioritize safety and cost-effectiveness to ensure external stability and internal strength under the static and dynamic forces [7-8]; in which external stability refers to soil failures such as overall instability, sliding failure, overturning failure, bearing capacity failure, and foundation settlement; meanwhile, internal strength involves preserving the structural integrity of retaining wall against maximum shear force and bending moments.

At present, domestic and foreign scholars have done much research on retaining walls. Excavation work inevitably leads to ground subsidence to some extent; to solve partial differential equations related to the plain strain problem, the separation of variables method (SVM) is used, the method assumes the movements of retaining wall as the given displacement boundary. An attempt is made to theoretically demonstrate the relationship between the movement of wall and the resulting ground subsidence. Comparisons between the present method, the elastoplastic finite element method, and in-situ measured data in soft soils, have been conducted to validate the accuracy of analytical solution [9]. A series of model tests were conducted to investigate the law of ground settlement caused by the movement of a rigid wall using different movement modes, namely translation mode (T mode), rotating around top mode (RT mode) and rotating around base mode (RB mode); the study successfully obtained distinct ground settlement curves for each movement mode. Under the T mode, a spoon-like settlement profile was observed, with the maximum surface settlement occurring at the wall back. In addition, the RT mode led to a

parabolic settlement profile, with the maximum surface settlement occurring at a specific distance away from the wall back. Finally, the RB mode resulted in a triangular settlement profile, again with the maximum surface settlement occurring at the wall back. The model tests revealed that different movement modes influenced the shape and location of the maximum surface settlement, which contributes to understand ground settlement induced by moving rigid walls [10]. Based on extensive experimental and numerical research conducted on geosynthetic-reinforced soil (GRS) retaining walls, an analytical method has been developed to accurately quantify the toe restraint of vertical GRS retaining walls under typical stress conditions. The approach utilizes Coulomb's active earth pressure theory to calculate the lateral earth pressure acting on the facing; additionally, a polygonal distribution is used to quantify the horizontal connection loads of the reinforcement layers. The method makes it possible to accurately assess the reinforcement loads of GRS retaining walls under working stress conditions, the serviceability of GRS retaining walls can be effectively analyzed in practical applications [11]. The active earth pressure acting on the flexible retaining wall is analyzed during excavation of foundation pit. The retaining wall is assumed to deflect in a bulge shape, with the maximum displacement occurring at the excavation surface. The slip surface is considered to be a plane passing through the wall toe. As the excavation depth increases, the angle of slip surface decreases, resulting in an expansion of the influence scope and the active earth pressure; the impact on the position of resultant force is minimal. When the excavation depth decreases, the soil friction angle and soil wall friction angle increase, the nonlinear distribution of active earth pressure becomes more obvious. The resultant force decreases, the distance between the action point of resultant force and the wall toe increases [12]. The soil slip surface characteristics are crucial for calculating earth pressure; laboratory model tests were conducted using non-cohesive sand to investigate the active and passive slip surface characteristics of the limited width soil behind a rigid wall. During the tests, the images of soil were collected and analyzed using the digital image correlation method, which can obtain displacement and shear strain of the soil in three movement modes: translation mode (T mode), rotating around top mode (RT mode), and rotating around base mode (RB mode). In addition, the passive earth pressure was tested on a removable retaining wall using a micro earth pressure gauge [13-15]. The distribution of earth pressure on a rigid retaining wall is strongly correlated with the mode of rotation and movement of wall. Analytical method considering displacement can be used to accurately calculate the distribution of active earth pressure when the wall movement is known. From the aspect of satisfying the requirements of overturning stability and eccentricity of wall base compressive stress, a method is proposed to determine the wall top displacement of active equilibrium condition and earth pressure distribution behind rigid retaining wall rotating about wall toe. Additionally, the impact of wall width and friction coefficient behind the retaining wall on the distribution of earth pressure is thoroughly analyzed [16]. Discrete element simulations considering various post-fill widths were carried out to investigate the distribution of active earth pressure in cohesionless soil under the rigid retaining wall rotating around the base mode (RB mode), the simulation results reveal that the distribution of active earth pressure in RB mode differs from the parabolic distribution of active earth pressure observed in translation mode (T mode). When the soil behind the wall is in an active limit state, multiple parallel slip lines are formed inside the soil. A novel oblique differential element method has been proposed based on the slicing of slip lines. In the case of infinite soils, the theoretical formula is consistent with the Coulomb's active earth pressure formula of triangular distribution. In the case of finite soils, the active earth pressure is piecewise linear distribution along with the depth. In the case of wall soil without friction, the theoretical formula will degenerate into Rankine's active earth pressure formula [17].

The application of recycled tire-derived aggregate (TDA) in combination with kaolin for retaining walls was investigated; the research examines the effects of TDA content on various geotechnical properties of TDA-kaolin specimens such as internal friction angle, maximum dry density (MDD), optimum moisture content (OMC), and saturated density (SD). The physical model experiments indicate that the highest level of elasticity was observed for the kaolin samples mixed with 60% shredded TDA in all tests at the moment of footing failure [18]. Failure surfaces are crucial in affecting active lateral earth thrusts on cantilever retaining walls. When determining the active earth thrust, it is essential to consider the intersection of failure surface and cantilever retaining wall. The calculation of lateral earth thrusts can differ depending on whether the wall has a short heel or a long heel, based on the intersection of cantilever wall and failure surface. The existing methods typically focus on only one particular case (either long heel or short heel), a new method for calculating lateral earth thrusts has been proposed, which can be applicable to cantilever walls with a short heel or long heel using the limit-equilibrium approach [19]. Conventional methods commonly utilized for calculating the active earth thrust on a retaining wall often neglect the friction between the soil and the wall. An analytical solution was proposed to accurately determine the active earth thrusts on a cantilever retaining wall with a short heel and a shear key supporting the granular backfill. Furthermore, the influence of wall dimensions and internal friction angles on the earth thrusts and failure surface angles were investigated [20]. The active earth pressure of inverted T-type retaining walls under rotational mode was investigated using a slip-line method. A typical failure mechanism was simulated with adaptive finite element software to verify the slip-line field calculation models for the inverted T-type retaining wall with a long or short heel. The stress state at each point was solved using the limit equilibrium method and the finite difference method. By converting the boundary conditions, the earth pressure acting on the stem and the second failure surface can be obtained [21-22]. The primary objective of designing reinforced concrete cantilever retaining wall structures is to prioritize safety measures against potential failures and compliance with standard building code requirements. To investigate the cost prediction of reinforced concrete cantilever retaining walls (RCCRWs), a comprehensive parametric study has been conducted by developing a specialized code optimized

using a metaheuristic-based algorithm, involving critical variables such as wall height, seismic zone, backfill material properties, and backfill inclination angle. It can be applied during the initial stages of a project, making a valuable contribution to determining approximate costs for RCCRW projects [23].

In this study, the finite element limit analysis software OptumG2 is used to analyze the deformation law, failure characteristics and mechanical mechanism of the sliding surface in the backfill, and the stability safety factor of inverted T-type retaining wall in an active limit state. In addition, analyzing influencing factors affecting inverted T-type retaining wall stability is an essential aspect of engineering implementation; there are many studies on influencing factors affecting inverted T-type retaining wall stability domestically and internationally, but the influencing factors for different slopes are different. In order to study the influence of inverted T-type retaining wall structure parameters, soil physical and soil mechanical parameters on the stability safety factor, this article considers the effect of eleven influencing factors, including the wall stem height, the bottom plate thickness, the wall heel width, the wall stem entirely vertical width, the wall toe width, the base angle of retaining wall, the soil cohesion, the soil internal friction angle, the soil young's modulus, the soil pisson's ratio and the soil unit weight. With the help of numerical simulation software OptumG2, an orthogonal experimental design is used to calculate the stability of an inverted T-type retaining wall in an active limit state under different working conditions based on the strength reduction method. The influence order of the inverted T-type retaining wall structural parameters, soil physical and soil mechanical parameters on the stability safety factor can be obtained, which provides a reference for the design and construction of inverted T-type retaining wall.

II. Failure Mechanism Analysis Against Inverted T-type Retaining Wall

A. Descriptions of inverted T-type retaining wall

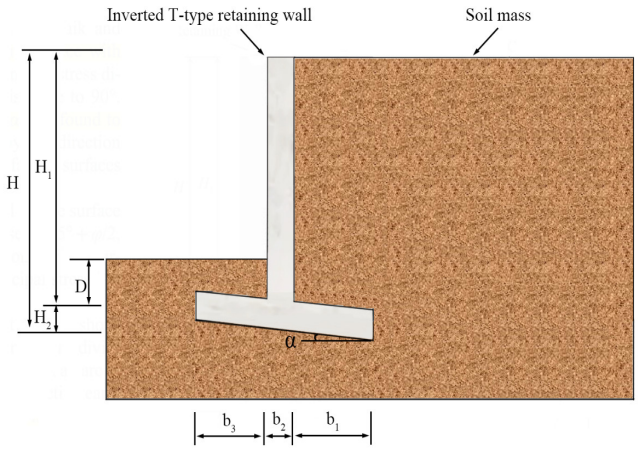

Fig.1. The geometry section of inverted T-Type retaining wall

The inverted T-type retaining wall is primarily supported by the combined resistance of the wall stem and the backfill on the bottom plate against the lateral earth pressure. The deformation law, failure characteristics and mechanical mechanism of the sliding surface in the backfill, and the stability safety factor of inverted T-type retaining wall are distinct from those of gravity retaining wall and reinforced earth retaining wall. The geometry section of inverted T-type retaining wall is illustrated in Fig.1. It is denoted that the retaining wall has a total height of H, with the wall stem height H_1. The bottom plate haves a thickness of H_2, which is buried to a depth of D at the bottom of wall stem. The wall heel width is designated as b_1, the wall stem is entirely vertical and has a width of b_2, and the wall toe width is designated as b_3. The base angle of retaining wall is represented as α.

B. Finite Element Model

(1) Introduction to finite element limit analysis software OptumG2

OptumG2 is advanced geotechnical analysis software that combines two-dimensional finite element analysis with limit analysis, making it a powerful tool for various applications. OptumG2 has multiple features, including user-friendly operation, fast modeling, support for CAD file import, and automatic grid encryption. OptumG2 is particularly effective in analyzing complex geological conditions, conducting failure analysis of intricate retaining structures, assessing foundation bearing capacity, and performing reliability analysis [24-25].

Unlike typical finite element programs, OptumG2 effortlessly handles convergence issues, eliminating the need for time-consuming algorithm parameter adjustments. OptumG2 streamlines the process by calculating strict upper and lower limits for the desired physical quantities, enabling users to estimate the exact solution and the associated error range immediately. Increasing the number of elements in the calculation makes the solution and the error estimation more accurate. OptumG2 offers adaptive grid encryption for analysis, resulting in high accuracy at a low computational cost.

(2) Finite element model and boundary state

This paper utilized the finite element limit analysis software OptumG2 to investigate the active failure mechanism of an inverted T-type retaining wall in the active limit state. The finite element model and adaptive mesh can be seen in Fig. 2, to eliminate boundary effects, the dimensions of finite element model are set as 24m in the horizontal direction and 12m in the vertical direction. The left and right sides of model are constrained in the normal direction, the bottom of model is constrained in both the tangential and normal directions, and the upper boundary of model is free. In order to achieve accurate engineering representation, the inverted T-type retaining wall is simulated using rigid elements with a unit weight of γ=25KN/m^3, the soil mass is simulated using the Mohr-Coulomb model. The retaining wall height H=6m; the wall stem height H_1=5.5m; the bottom plate thickness H_2=0.5m; the buried depth at the bottom of wall stem D=1m; the wall heel width b_1=1m; the wall stem is entirely vertical with a width of b_2=0.5m; the wall toe width is b_3=1m and the base angle of retaining wall α =15^o.

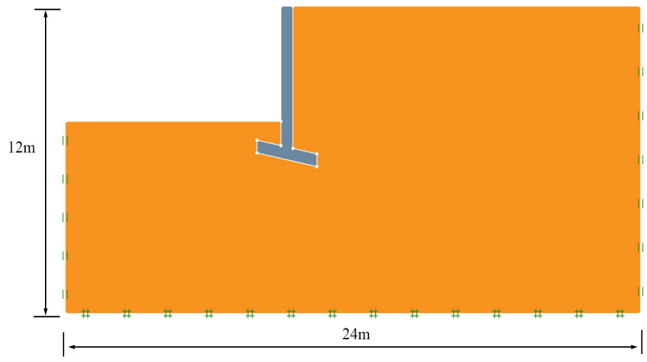

(a) Finite element mode

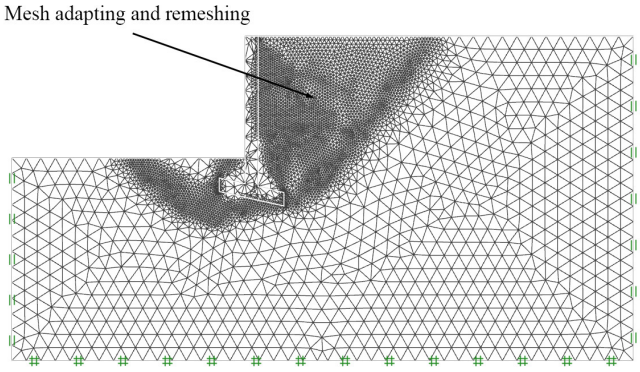

(b) Adaptively mesh

Fig.2. The finite element model and adaptively mesh

(3) Numerical calculation settings and material parameters

The mesh is redistributed through adaptive iterations to achieve a more accurate distribution. The upper and lower bound limit elements are carefully selected in the finite element model; it is noted that the influence of elements number in upper and lower bound limit becomes negligible when the number of elements exceeds 25000. Consequently, three adaptive iterations are conducted with considering shear dissipation as the control variable, an initial mesh of 5000 elements is used and the total number of mesh elements is refined to 25000 for the model in this numerical analysis.

The Mohr-Coulomb model is used in the finite element model to simulate the soil behavior. The main parameters of the backfill are presented in Table I. The soil is assumed to fill in a normally consolidated state. The dilatancy angle of soil is set to 0, and the soil adheres to the non-correlated flow criterion.

TABLE I
THE MAIN CALCULATION PARAMETERS OF SOIL MASS

Name of soil layer	Natural unit weight (kg/m^3)	Cohesion (kPa)	Internal friction angle (°)	Young's modulus (MPa)	Poisson's ratio
Firm clay	22	16	20	25	0.25

C. Calculation principle of strength reduction method

The safety factor is a useful criterion for evaluating the stability of an inverted T-type retaining wall and is commonly used in stability analyses. It can be defined as the extent to which the shear strength of soil decreases when the retaining wall reaches the critical failure state [26].

To determine the safety factor F_s of the inverted T-type retaining wall, the shear strength index c , φ is systematically reduced divided by the reduction coefficient F_s', thereby obtaining a new set of shear strength index c' , φ' . Subsequently, the finite element analysis is carried out with repeated calculations until the inverted T-type retaining wall reaches the critical failure state. At this moment, the safety factor F_s of the inverted T-type retaining wall corresponds to the ratio of the original shear strength index c , φ of the soil to the utilized shear strength index c_f , φ_f of the soil:

$$F_s = \frac{\tan\varphi}{\tan\varphi_f} = \frac{c}{c_f} \tag{1}$$

where F_s is the safety factor of inverted T-type retaining wall; c and φ are the original soil cohesion and original soil internal friction angle; c_f and φ_f are the soil cohesion and soil internal friction angle after strength reduction in critical failure state.

By comparing the definition of safety factor between the Bishop method and the strength reduction method, it can be concluded that both methods have the same physical meaning for the safety factor. The strength reduction method aligns with the traditional method; it has the advantages of clarity and simplicity in the calculation principle.

D. The criteria for retaining wall stability calculation and judgment

As shown in Table II and Table III, the criteria for calculating and assessing the stability of retaining wall are defined in the national standard "Technical Code for Construction Slope Engineering" (GB50330-2013) [27]. If a safety accident that may occur can lead to severe consequences, the safety grade for slope engineering is categorized as First order; under normal conditions, the critical safety factor F_{st} for permanent slopes should be considered as 1.35.

E. Numerical simulation and mechanism analysis of inverted T-type retaining wall failure process

The strength reduction method is utilized to investigate the failure behavior of an inverted T-type retaining wall and evaluate its safety factor. The stability analysis of soil mass is conducted using the Mohr-Coulomb constitutive equation, which can effectively describes the stress and strain of soil mass, and the required parameters can be easily obtained [28].

During the numerical simulation process, the instability of the inverted T-type retaining wall occurs gradually, starting from localized deformation accumulation, gradual expansion of regional instability, and eventually leading to large deformation and overall failure. The sliding process of inverted T-type retaining wall in active limit state can be visualized through shear dissipation contours; the shear

dissipation contour represents the potential sliding surface. The intensity of shear dissipation energy increases, as indicated by the redder color in the figure, implying a higher possibility of shear occurring in the corresponding region.

When the retaining wall height H=6m, the wall stem height H_1=5.5m, the bottom plate thickness H_2 =0.5m, the buried depth at the bottom of the wall stem D=1m, the wall heel width b_1=1m, the wall stem is entirely vertical with a width of b_2=0.5m, the wall toe width is b_3=1m and the base angle of the retaining wall α =15°; the soil parameters are selected as shown in Table I, the shear dissipation contours and normalized displacement contours for sliding process of inverted T-type retaining wall in the active limit state is shown in Fig.3 and Fig.4, respectively.

TABLE II
CLASSIFICATION OF SLOPE STABILITY STATES

Slope type		Safety grade of slope engineering		
		First order	Second order	Third order
Permanent slope	Normal condition	1.35	1.30	1.25
	Seismic condition	1.15	1.10	1.05
Temporary slope		1.25	1.20	1.15

TABLE III
CRITICAL SAFETY FACTOR OF SLOPE F_{ST}

Slope stability coefficient F_s	$F_s < 1.00$	$1.00 \le F_s < 1.05$	$1.00 \le F_s < F_{st}$	$F_s \ge F_{st}$
Slope stability states	Unstable	Understable	Basically stable	Stable

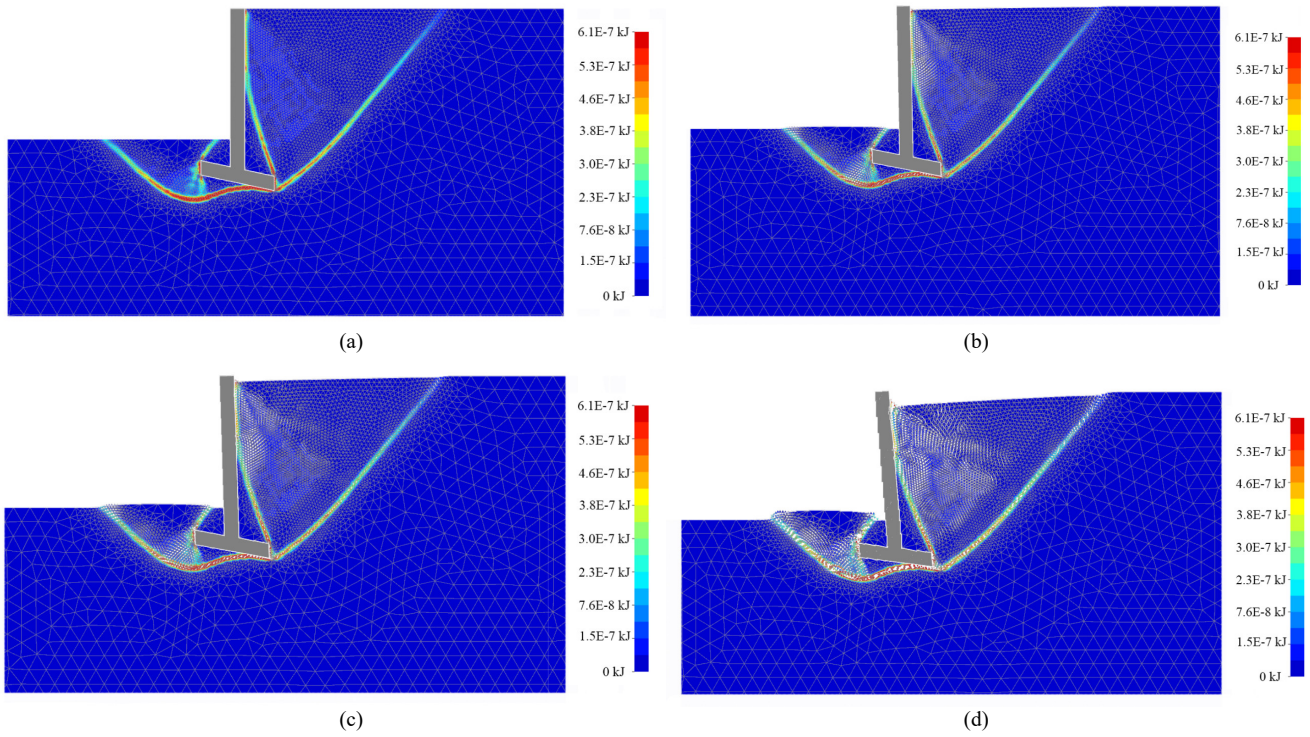

Fig. 3. Shear dissipation contours for sliding process of inverted T-type retaining wall in active limit state

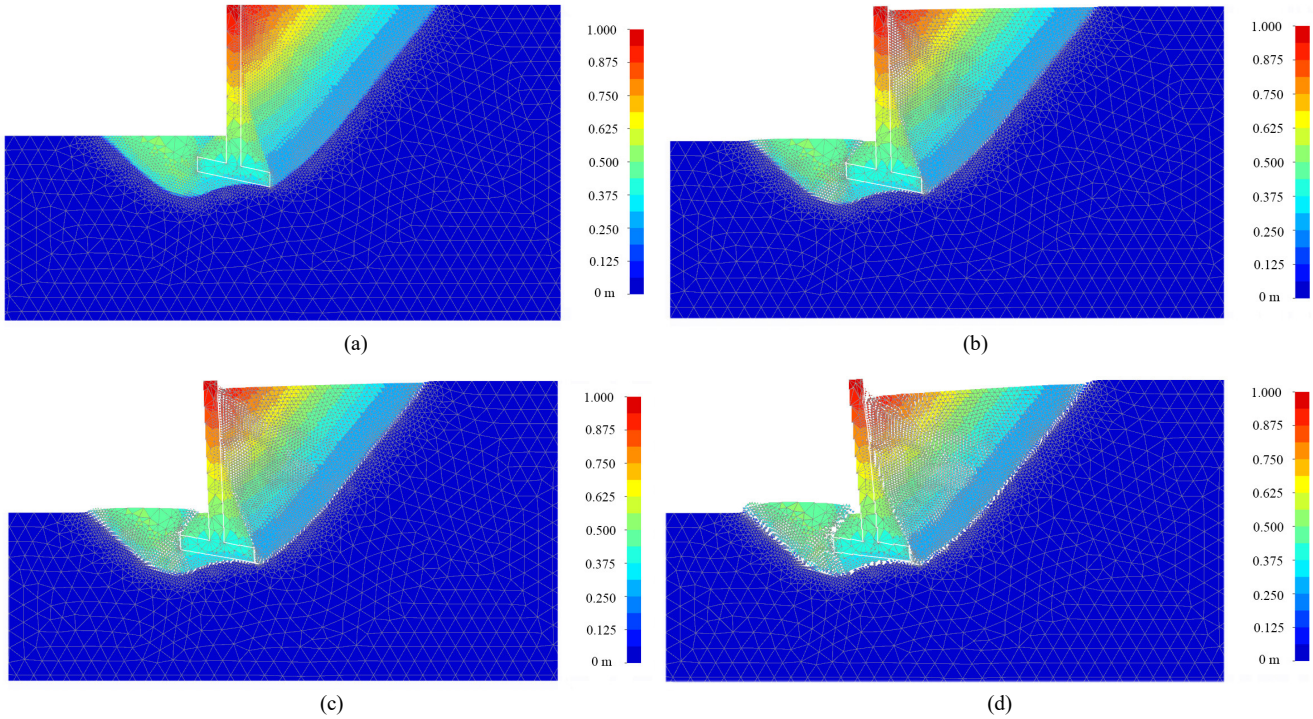

Fig. 4. Normalized displacement contours for sliding process of inverted T-type retaining wall in active limit state

Two sliding failure surfaces developed in the soil behind the inverted T-type retaining walls in an active state are called the first and second failure surfaces behind the wall, respectively. The first failure surface developed from the lower edge of wall bottom plate to the ground, and the second failure surface formed from the upper edge of wall bottom plate to the wall stem. A sliding failure surface in the soil in front of the inverted T-type retaining wall develops from the bottom of wall heel to the ground. The inverted T-type retaining wall is characteristic of overturning failure; the soil displacement maximum for the sliding process of the inverted T-type retaining wall is located near the top of wall.

III. Parameter Analysis of Influencing Factors for Safety Factor of Inverted T-Type Retaining Wall

A. Orthogonal experimental design scheme and numerical simulation test results

As shown in Fig.2, the finite element model and adaptively mesh of an inverted T-type retaining wall are established based on the finite element limit analysis software OptumG2.

For the parameter analysis of influencing factors for the safety factor of inverted T-type retaining wall, eleven influencing factors that affect the stability of retaining wall are chosen as follows: the wall stem height, the bottom plate thickness, the wall heel width, the wall stem entirely vertical width, the wall toe width, the base angle of retaining wall, the soil cohesion, the soil internal friction angle, the soil young's modulus, the soil pisson's ratio, and the soil unit weight. Each influencing factor is selected at five levels based on engineering practice experience. A correlation of the investigated range of inverted T-type retaining wall structure parameters, soil physical and soil mechanical parameters in accordance with conventional values for slope design would be insightful; the values of inverted T-type retaining wall structure parameters, soil physical and soil mechanical parameters are determined according to the engineering geological manual on soil properties [29] and the relevant retaining wall papers [30-32]. If a comprehensive combination test is conducted, 5^{11}=48828125 tests are required; Due to the limitations of time and money, it is impossible and unnecessary to perform 48828125 tests.

By utilizing the orthogonal table for test arrangement, the number of tests can be significantly minimized while ensuring a comprehensive understanding of the impact of multiple influencing factors on the target index. The orthogonal design method effectively addresses the issues of limited perspective and distorted test results that arise from reducing influencing factors solely based on subjective experiences. Therefore, the orthogonal design method can allow for the analysis of the range and variance of different influencing factors that influence the stability of inverted T-type retaining walls, enabling the identification of significant influencing factors that play a crucial role in affecting the stability of the structure.

To determine the impact of eleven influencing factors on inverted T-type retaining wall stability, five horizontal values are used for each influencing factor to obtain an orthogonal design table L_{50} (5^{11}) [33]. The orthogonal analysis scheme of horizontal values for each influencing factor is shown in Table IV. The wall stem height is 3m, 4m, 5m, 6m and 7m, respectively; the bottom plate thickness is 0.5m, 0.625m, 0.75m, 0.875m and 1m, respectively; the wall heel width is 0.5m, 0.875m, 1.25m, 1.625m and 2m, respectively; the wall stem width is 0.5m, 0.625m, 0.75m, 0.875m and 1m, respectively; the wall toe width is 0.5m, 0.875m, 1.25m, 1.625m and 2m, respectively; the base angle of retaining wall is -30°, -15 °, 0, 15° and 30°, respectively; in which the positive sign indicates that the vertical normal direction of the base of retaining wall points to the inside of retaining wall, and the negative sign indicates that the vertical normal direction of the base of retaining wall points to the outside of retaining wall; the soil cohesion is 0kPa, 5kPa, 10kPa, 15kPa,

and 20kPa, respectively; the soil internal friction angles is 5°, 10°, 15°, 20° and 25°, respectively; the soil young's modulus is 10MPa, 20MPa, 30MPa, 40MPa and 50MPa, respectively; the soil pisson's ratio is 0.15, 0.2, 0.25, 0.3 and 0.35, respectively; the soil unit weight is 15kN/m^3, 17kN/m^3, 19kN/m^3, 21kN/m^3 and 23kN/m^3, respectively.

Stability calculations are performed on the 50 working conditions using the numerical simulation software OptumG2. The relationship between the safety factor and the changes in inverted T-type retaining wall structure parameters, soil physical and soil mechanical parameters are obtained; the numerical simulation test results of orthogonal experimental design for inverted T-type retaining wall stability analysis are shown in Table V, and the range analysis results of orthogonal tests are shown in Table VI.

TABLE IV
THE ORTHOGONAL ANALYSIS SCHEME OF HORIZONTAL VALUES FOR EACH INFLUENCING FACTOR

Horizontal values	Wall stem height (m)	Bottom plate thickness (m)	Wall heel width (m)	Wall stem width (m)	Wall toe width (m)	Base angle (°)	Soil cohesion (kPa)	Soil internal friction angle (°)	Soil young's modulus (MPa)	Soil pisson's ratio	Soil unit weight (kN/m^3)
1	3	0.5	0.5	0.5	0.5	-30	0	5	10	0.15	15
2	4	0.625	0.875	0.625	0.875	-15	5	10	20	0.2	17
3	5	0.75	1.25	0.75	1.25	0	10	15	30	0.25	19
4	6	0.875	1.625	0.875	1.625	15	15	20	40	0.3	21
5	7	1	2	1	2	30	20	25	50	0.35	23

TABLE V
NUMERICAL SIMULATION TEST RESULTS OF ORTHOGONAL EXPERIMENTAL DESIGN FOR INVERTED T-TYPE RETAINING WALL STABILITY ANALYSIS

Test number	Wall stem height (m)	Bottom plate thickness (m)	Wall heel width (m)	Wall stem width (m)	Wall toe width (m)	Base angle (°)	Soil cohesion (kPa)	Soil internal friction angle (°)	Soil young's modulus (MPa)	Soil pisson's ratio	Soil unit weight (kN/m^3)	Safety factor F_s
1	3	0.5	0.5	0.5	0.5	-30	0	5	10	0.15	15	0.49
2	3	0.625	0.875	0.625	0.875	-15	5	10	20	0.2	17	1.45
3	3	0.75	1.25	0.75	1.25	0	10	15	30	0.25	19	2.63
4	3	0.875	1.625	0.875	1.625	15	15	20	40	0.3	21	4.38
5	3	1	2	1	2	30	20	25	50	0.35	23	5.85
6	4	0.5	0.875	0.75	1.625	30	0	10	30	0.3	23	0.71
7	4	0.625	1.25	0.875	2	-30	5	15	40	0.35	15	1.49
8	4	0.75	1.625	1	0.5	-15	10	20	50	0.15	17	2.11
9	4	0.875	2	0.5	0.875	0	15	25	10	0.2	19	2.86
10	4	1	0.5	0.625	1.25	15	20	5	20	0.25	21	2.15
11	5	0.5	1.25	1	0.875	15	15	5	30	0.35	17	1.57
12	5	0.625	1.625	0.5	1.25	30	20	10	40	0.15	19	2.26
13	5	0.75	2	0.625	1.625	-30	0	15	50	0.2	21	0.81
14	5	0.875	0.5	0.75	2	-15	5	20	10	0.25	23	1.21
15	5	1	0.875	0.875	0.5	0	10	25	20	0.3	15	1.72
16	6	0.5	1.625	0.625	2	0	20	15	10	0.3	17	1.91
17	6	0.625	2	0.75	0.5	15	0	20	20	0.35	19	0.93
18	6	0.75	0.5	0.875	0.875	30	5	25	30	0.15	21	1.28
19	6	0.875	0.875	1	1.25	-30	10	5	40	0.2	23	0.91
20	6	1	1.25	0.5	1.625	-15	15	10	50	0.25	15	1.29

TABLE V
NUMERICAL SIMULATION TEST RESULTS OF ORTHOGONAL EXPERIMENTAL DESIGN FOR INVERTED T-TYPE RETAINING WALL STABILITY ANALYSIS

Test number	Wall stem height (m)	Bottom plate thickness (m)	Wall heel width (m)	Wall stem width (m)	Wall toe width (m)	Base angle (°)	Soil cohesion (kPa)	Soil internal friction angle (°)	Soil young's modulus (MPa)	Soil pisson's ratio	Soil unit weight (kN/m^3)	Safety factor F_s
21	7	0.5	2	0.875	1.25	-15	15	15	20	0.15	23	1.71
22	7	0.625	0.5	1	1.625	0	20	20	30	0.2	15	1.96
23	7	0.75	0.875	0.5	2	15	0	25	40	0.25	17	1.31
24	7	0.875	1.25	0.625	0.5	30	5	5	50	0.3	19	0.21
25	7	1	1.625	0.75	0.875	-30	10	10	10	0.35	21	0.95
26	3	0.5	0.5	0.875	2	15	10	10	50	0.2	19	2.16
27	3	0.625	0.875	1	0.5	30	15	15	10	0.25	21	3.11
28	3	0.75	1.25	0.5	0.875	-30	20	20	20	0.3	23	3.43
29	3	0.875	1.625	0.625	1.25	-15	0	25	30	0.35	15	2.22
30	3	1	2	0.75	1.625	0	5	5	40	0.15	17	1.99
31	4	0.5	0.875	0.5	1.25	0	5	20	50	0.35	21	1.01
32	4	0.625	1.25	0.625	1.625	15	10	25	10	0.15	23	2.78
33	4	0.75	1.625	0.75	2	30	15	5	20	0.2	15	2.49
34	4	0.875	2	0.875	0.5	-30	20	10	30	0.25	17	2.17
35	4	1	0.5	1	0.875	-15	0	15	40	0.3	19	0.89
36	5	0.5	1.25	0.75	0.5	-15	20	25	40	0.2	21	2.31
37	5	0.625	1.625	0.875	0.875	0	0	5	50	0.25	23	0.21
38	5	0.75	2	1	1.25	15	5	10	10	0.3	15	1.69
39	5	0.875	0.5	0.5	1.625	30	10	15	20	0.35	17	1.72
40	5	1	0.875	0.625	2	-30	15	20	30	0.15	19	2.61
41	6	0.5	1.625	1	1.625	-30	5	25	20	0.25	19	1.45
42	6	0.625	2	0.5	2	-15	10	5	30	0.3	21	1.32
43	6	0.75	0.5	0.625	0.5	0	15	10	40	0.35	23	0.63
44	6	0.875	0.875	0.75	0.875	15	20	15	50	0.15	15	2.18
45	6	1	1.25	0.875	1.25	30	0	20	10	0.2	17	1.32
46	7	0.5	2	0.625	0.875	30	10	20	40	0.25	23	1.77
47	7	0.625	0.5	0.75	1.25	-30	15	25	50	0.3	17	1.41
48	7	0.75	0.875	0.875	1.625	-15	20	5	10	0.35	19	1.11
49	7	0.875	1.25	1	2	0	0	10	20	0.15	21	0.42
50	7	1	1.625	0.5	0.5	15	5	15	30	0.2	23	0.64

B. Numerical simulation results analysis and discussion

As the number of experiments significantly reduced, it is crucial to choose an appropriate analysis method for the orthogonal experimental data. Range analysis is commonly conducted to reveal the main influencing factors impacting the target index.

Range analysis aims to assess the impact of different influencing factors on the target index. Two crucial parameters in range analysis are K_{ji} and R_j. K_{ji} represents the sum of the evaluation index at all levels (i, i=1, 2, 3, 4, 5) for each influencing factor (j, j=A, B, C, D, E, F, G, H, I, J, K). Meanwhile, $\overline{K}_{ji}$ refers to the average value of K_{ji}. R_j is the

TABLE VI
RANGE ANALYSIS RESULTS OF THE ORTHOGONAL TESTS

Horizontal values	Wall stem height (m)	Bottom plate thickness (m)	Wall heel width (m)	Wall stem width (m)	Wall toe width (m)	Base angle (°)	Soil cohesion (kPa)	Soil internal friction angle (°)	Soil young's modulus (MPa)	Soil pisson's ratio	Soil unit weight (kN/m^3)
Average of indicators $\overline{K}_1$	2.77	1.51	1.39	1.63	1.43	1.57	0.93	1.25	1.74	1.78	1.73
Average of indicators $\overline{K}_2$	1.87	1.69	1.61	1.65	1.66	1.56	1.24	1.37	1.75	1.69	1.70
Average of indicators $\overline{K}_3$	1.61	1.75	1.74	1.68	1.73	1.53	1.81	1.71	1.71	1.73	1.71
Average of indicators $\overline{K}_4$	1.32	1.83	1.86	1.76	1.82	1.98	2.21	2.07	1.79	1.77	1.77
Average of indicators $\overline{K}_5$	1.15	1.94	2.11	2.00	2.08	2.07	2.53	2.32	1.72	1.75	1.81
Extreme difference R	1.62	0.43	0.72	0.37	0.65	0.54	1.60	1.07	0.08	0.09	0.11

range between the maximum and minimum values of $\overline{K}_{ji}$, which is utilized to determine the significance of influencing factor [33]. The calculation of R_j is as follows:

$$R_j = \max\left\{\overline{K}_{ij}\right\} - \min\left\{\overline{K}_{ij}\right\} \quad (2)$$

In range analysis, a larger value of R_j indicates a more substantial influence of the influencing factor on the target index; therefore, the corresponding influencing factor is considered an important influencing factor.

The relationship between the safety factor of inverted T-type retaining wall and the wall stem height, the bottom plate thickness, the wall heel width, the wall stem entirely vertical width, the wall toe width, the base angle of retaining wall, the soil cohesion, the soil internal friction angle, the soil young's modulus, the soil pisson's ratio and the soil unit weight are shown in Fig. 5~ Fig. 15, respectively.

From Table VI and Fig.5~ Fig.15, it is evident that there is a rapid decrease for the safety factor of retaining wall as the wall stem height increases from 3m to 4m, dropping from 2.77 to 1.87; when the wall stem height increases from 4m to 7m, the safety factor of retaining wall decreases approximately linearly from 1.87 to 1.15. As the bottom plate thickness increases from 0.5m to 1m, there is an approximately linear increment for the safety factor of retaining wall from 1.51 to 1.94. Likewise, with an increment in wall heel width from 0.5m to 2m, the safety factor of retaining wall shows an approximately linear increment from 1.39 to 2.11. Furthermore, when the wall stem width increases from 0.5m to 0.875m, there is a linear increment for the safety factor of retaining wall from 1.63 to 1.76; as the wall stem width increases from 0.875m to 1m, the safety factor of retaining wall experiences a greater increment from 1.76 to 2.00. Additionally, an increment in wall toe width from 0.5m to 2m leads to an approximately linear increment in the safety factor of retaining wall from 1.43 to 2.08. When the base angle varies from -30^o to 0, there is a slight decrease for the safety factor of retaining wall from 1.57 to 1.53; when the base angle varies from 0 to 30^o, the safety factor of retaining wall significantly grows from 1.57 to 2.07. It shows that the base angle should be designed at about 30^o, which is helpful to the stability of retaining wall. Moreover, an increment in the soil cohesion from 0 to 20kPa results in an approximately linear increment for the safety factor of retaining wall from 0.93 to 2.53. As the internal friction angle of soil increases from 5^o to 25^o, there is an approximately linear increment for the safety factor of retaining wall from 1.25 to 2.32. Lastly, as the soil young's modulus increases from 10MPa to 50MPa, the soil poisson's ratio increases from 0.15 to 0.35, and the soil unit weight increases from 15kN/m^3 to 23kN/m^3, the safety factor of retaining wall remains almost unchanged within the ranges of 1.71 to 1.79, 1.69 to 1.78, and 1.70 to 1.81, respectively.

The extreme difference R in the orthogonal experimental analysis table reflects equilibrium, and the size of extreme difference R reflects the influence of the influencing factor change on the experimental target index. The extreme difference R of the wall stem height, the bottom plate thickness, the wall heel width, the wall stem entirely vertical width, the wall toe width, the base angle of retaining wall, the soil cohesion, the soil internal friction angle, the soil young's modulus, the soil pisson's ratio and the soil unit weight for the safety factor of retaining wall are 1.62, 0.43, 0.72, 0.37, 0.65, 0.54, 1.60, 1.07, 0.08, 0.09, and 0.11, respectively. According to the order of range, the primary and secondary relationships of various influencing factors are arranged from the largest to the smallest; the order of influencing factors on the safety factor of retaining wall is as follows: wall stem height, soil cohesion, soil internal friction angle, wall heel width, wall toe width, base angle, bottom plate thickness, wall stem width, soil unit weight, soil pisson's ratio and soil young's modulus. The increment in wall stem height will decrease retaining wall safety and cause the retaining structure to fail. Increasing soil cohesion, soil internal friction angle, wall heel width, wall toe width, base angle, bottom plate thickness, and wall stem width in retaining wall design can effectively improve the safety of retaining wall. The change in soil young's modulus, soil poisson's ratio, and soil unit weight will not significantly impact the stability of retaining wall.

It should be pointed out that the order of influencing factor on the safety factor of a retaining wall may be different because the influencing factor levels are determined in different ranges; the influencing factor levels should be selected based on the actual used values of retaining wall design.

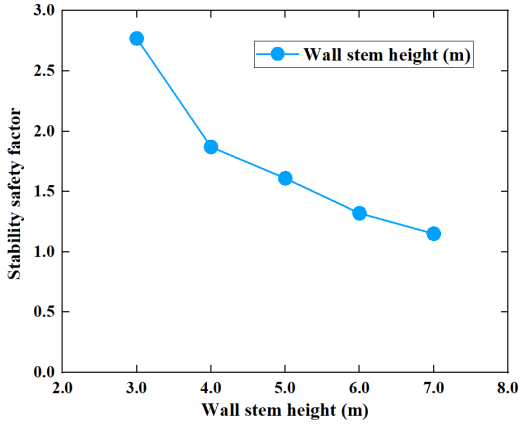

Fig. 5. The relationship between the safety factor of retaining wall and the wall stem height

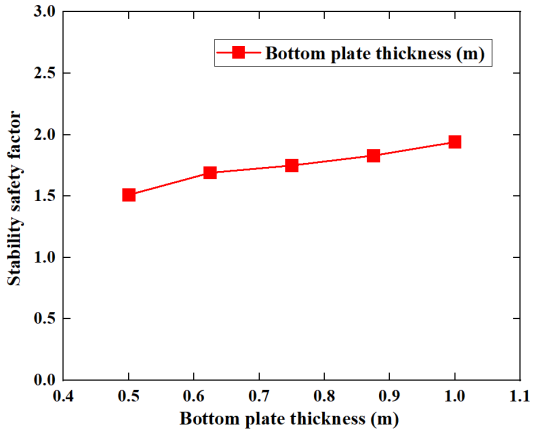

Fig. 6. The relationship between the safety factor of retaining wall and the bottom plate thickness

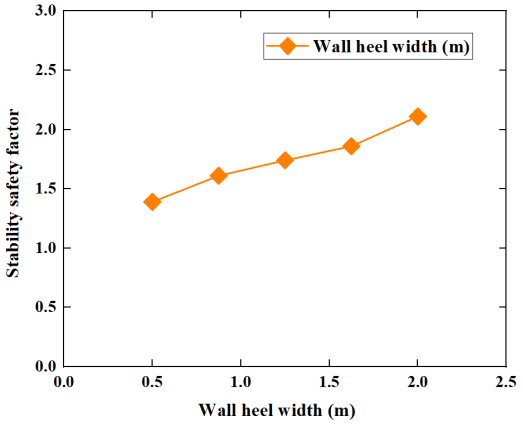

Fig .7. The relationship between the safety factor of retaining wall and the wall heel width

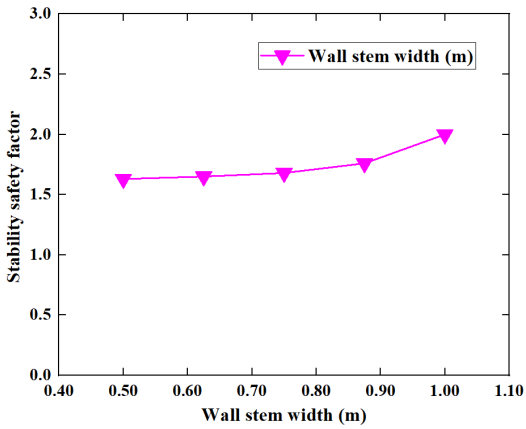

Fig. 8. The relationship between the safety factor of retaining wall and the wall stem entirely vertical width

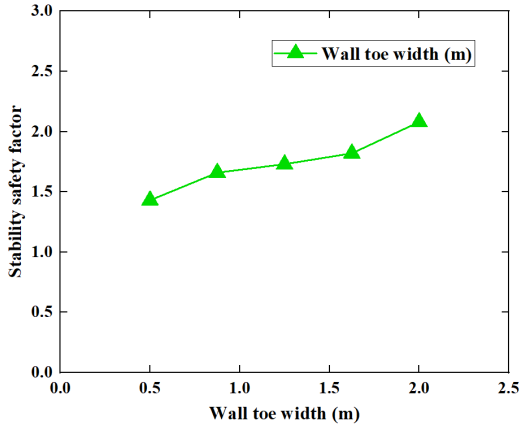

Fig. 9. The relationship between the safety factor of retaining wall and the wall toe width

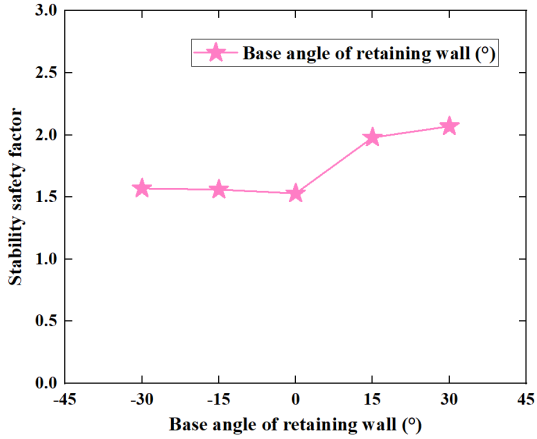

Fig. 10. The relationship between the safety factor of retaining wall and the base angle of retaining wall

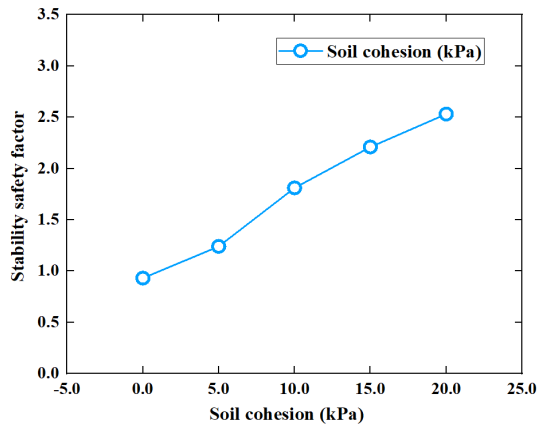

Fig. 11. The relationship between the safety factor of retaining wall and the soil cohesion

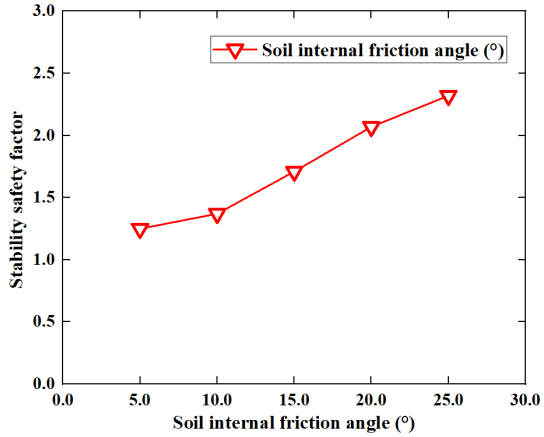

Fig .12. The relationship between the safety factor of retaining wall and the soil internal friction angle

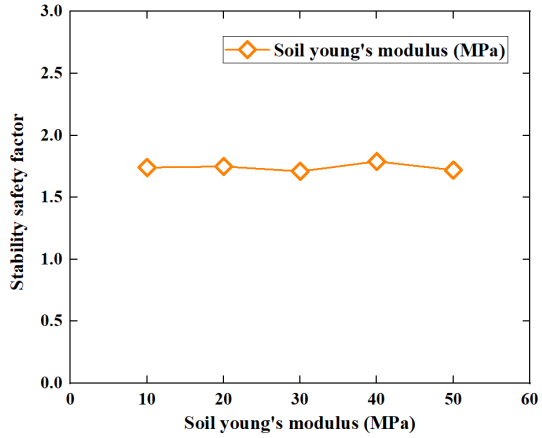

Fig. 13. The relationship between the safety factor of retaining wall and the soil young's modulus

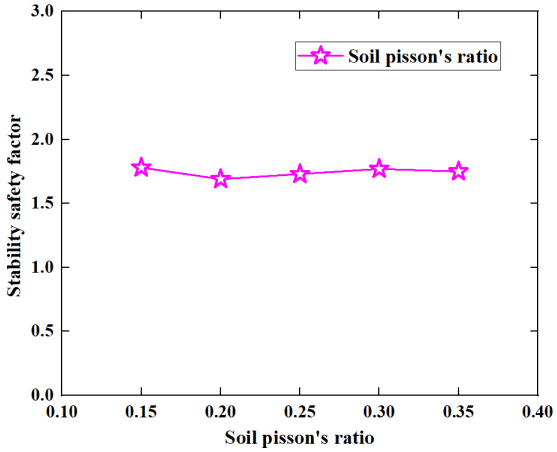

Fig. 14. The relationship between the safety factor of retaining wall and the soil pisson's ratio

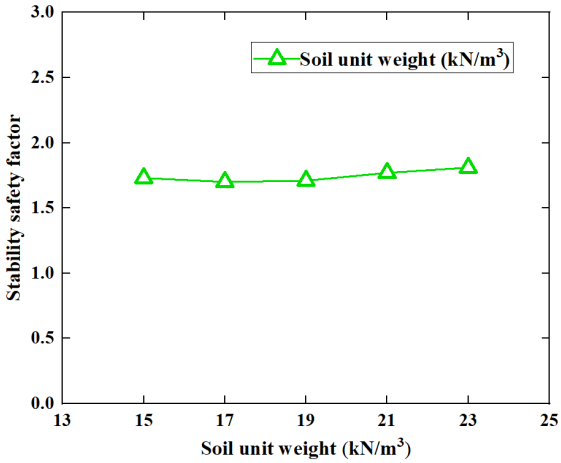

Fig. 15. The relationship between the safety factor of retaining wall and the soil unit weight

IV. Conclusion

In this study, the finite element limit analysis software OptumG2 is used to analyze the deformation law, failure characteristics and mechanical mechanism of the sliding surface in the backfill, and stability safety factor of inverted T-type retaining wall in an active limit state. With the help of numerical simulation software OptumG2, an orthogonal experimental design is used to calculate the stability of inverted T-type retaining wall in an active limit state under different working conditions based on the strength reduction method. The main conclusions are drawn as follows:

1) Two sliding failure surfaces are developed in the soil behind the inverted T-type retaining walls in an active state; which are called the first and second failure surfaces behind the wall, respectively. The first failure surface developed from the lower edge of the wall bottom plate to the ground, and the second failure surface formed from the upper edge of the wall bottom plate to the wall stem. A sliding failure surface in the soil in front of the inverted T-type retaining wall develops from the bottom of the wall heel to the ground. The inverted T-type retaining wall has the characteristic of overturning failure; the soil displacement maximum for the sliding process of the inverted T-type retaining wall is located near the top of wall.

2) As the wall stem height increases from 3m to 4m, the safety factor of retaining wall rapidly decreases from 2.77 to 1.87; when the wall stem height increases from 4m to 7m, the safety factor of soil slope decreases approximately linearly from 1.87 to 1.15. As the bottom plate thickness increases from 0.5m to 1m, the safety factor of retaining wall increases approximately linearly from 1.51 to 1.94. As the wall heel width increases from 0.5m to 2m, the safety factor of retaining wall increases approximately linearly from 1.39 to 2.11. As the wall stem width increases from 0.5m to 0.875m, the safety factor of retaining wall increases approximately linearly from 1.63 to 1.76; as the wall stem width increases from 0.875m to 1m, the safety factor of retaining wall greater increases from 1.76 to 2.00. As the wall toe width increases from 0.5m to 2m, the safety factor of retaining wall increases approximately linearly from 1.43 to 2.08. When the base angle of retaining wall vary from -30° to 0, the safety factor of retaining wall drop slightly from 1.57 to 1.53; meanwhile, when the base angle of retaining wall vary from 0 to 30°, the safety factor of retaining wall grows significantly from 1.57 to 2.07. As the cohesion of soil increases from 0 to 20kPa, the safety factor of retaining wall increases approximately linearly from 0.93 to 2.53. As the internal friction angle of soil increases from 5° to 25°, the safety factor of retaining wall increases approximately linearly from 1.25 to 2.32. As the soil young's modulus of soil increases from 10MPa to 50MPa, soil pisson's ratio increases from 0.15 to 0.35, the unit weight of soil increases from 15kN/m^3 to 23kN/m^3, the safety factor of retaining wall almost unchanged with the range from 1.71 to 1.79, from 1.69 to 1.78 and from 1.70 to 1.81, respectively.

3) The safety factor of a retaining wall is influenced by various influencing factors, including wall stem height, bottom plate thickness, wall heel width, wall stem width, wall toe width, base angle, soil cohesion, soil internal friction angle, soil young's modulus, soil pisson's ratio, and soil unit weight. The extreme difference R of these influencing factors is as follows: 1.62, 0.43, 0.72, 0.37, 0.65, 0.54, 1.60, 1.07, 0.08, 0.09, and 0.11, respectively. From largest to smallest, the order of influencing factors on the safety factor of retaining wall is as follows: wall stem height, soil cohesion, soil internal friction angle, wall heel width, wall toe width, base angle, bottom plate thickness, wall stem width, soil unit weight, soil pisson's ratio, and soil young's modulus. The increment in wall stem height will decrease the safety factor of retaining wall and may lead to structural failure. Increasing soil cohesion, soil internal friction angle, wall heel width, wall toe width, base angle, bottom plate thickness, and wall stem width can effectively improve the safety of retaining

wall. The changes in soil young's modulus, soil pisson's ratio, and soil unit weight do not significantly impact the stability of retaining wall.

The stability analysis of inverted T-type retaining wall in active limit state is a complex scientific problem. The strength reduction method and orthogonal experimental design can correctly obtain the influencing factors sensitivity of stability analysis for inverted T-type retaining wall in active limit state, help distinguish between primary and secondary influencing factors, and provide a reliable basis for optimizing inverted T-type retaining wall design. Through sensitivity analysis of stability influencing factors for inverted T-type retaining walls in the active limit state based on the strength reduction method and orthogonal experimental design, the study provides a valuable reference for studying the failure laws and stability of retaining walls, which is beneficial to the design and construction of inverted T-type retaining wall design.

REFERENCES

[1] Y. W. Hong, "Research review on slide - resistance of shear key in retaining walls," Yangtze River, vol. 53, no. 4, pp 135-143, 2022.

[2] X. X. Zhang, S. M. He, and X. Y. Fan, "Seismic stability of L-shape retaining walls and determination method of sliding surface," Rock and Soil Mechanics, vol. 40, no. 10, pp 4011-4020, 2019.

[3] Z. H. Li, and S. G. Xiao, "Calculation method for seismic permanent displacement of cantilever retaining walls considering different movement modes," Rock and Soil Mechanics, vol. 42, no. 3, pp 723-734, 2021.

[4] S. B. Jo, J. G. Ha, J. S. Lee, and D. S. Kim, "Evaluation of the seismic earth pressure for inverted T-shape stiff retaining wall in cohesionless soils via dynamic centrifuge," Soil Dynamics and Earthquake Engineering, vol. 92, no. 1, pp 1-13, 2017.

[5] J. H. Zhang, H. R. Hu, W. Fu, , J. H. Peng, F. Li, and L. Ding, "Method for efficient calculating earth pressure of retaining wall considering plant transpiration," Scientific Reports, vol. 13, no.1, pp 1-16, 2023.

[6] W. D. Hu, Y. Q. Zeng, X. N. Zhu, and T. Hu, "Determination of passive earth pressure on a cantilever retaining wall in a narrow foundation pit based on logarithmic spiral sliding surface," International Journal of Geomechanics, vol. 23, no. 8, pp 1-9, 2023.

[7] X. N. Zhu, Y. Q. Zeng, W. D. Hu, X. H. Liu, and X. Y. Zhou, "Experimental study on passive earth pressure against flexible retaining wall with drum deformation," Engineering Letters, vol. 29, no. 2, pp 339-350, 2021.

[8] X. N. Zhu, W. D. Hu, Y. Q. Zeng, T. Hu, S. Q. Jiang, and W. W. Wang. " Experimental study on deformation characteristics and active earth pressure against the flexible retaining wall with limited width soil in foundation pit," IAENG International Journal of Applied Mathematics, vol. 52, no. 4, pp 875-889, 2022.

[9] J. G. Qian, and W. Q. Wang, "Analytical solutions to ground settlement induced by movement of rigid retaining wall," Chinese Journal of Rock Mechanics and Engineering, vol. 32, no. Supp.1, pp 2698-2703, 2013.

[10] R. Z. Zhang, and J. G. Qian, "Model tests on excavation-induced ground settlement due to movement of retaining wall," Rock and Soil Mechanics, vol. 36, no. 10, pp 2921-2926, 2015.

[11] H. B. Liu, G. Q. Yang, and C. Hung, "Analyzing reinforcement loads of vertical geosynthetic-reinforced soil walls considering toe restraint," International Journal of Geomechanics, vol. 17, no. 6, pp. 1-11, 2017.

[12] M. L. Liu, Y. J. Hou, D. L. Zhang, and Q. Fang, "Research on active earth pressure of flexible retaining wall considering construction effect of foundation pit in sandy soil," Rock and Soil Mechanics, vol. 39, no. Supp.1, pp 149-158, 2018.

[13] C. Y. Wang, X. P. Liu, J. Q. Zhang, and Z. H. Cao, "Experimental study on passive slip surface of limited width soil behind a rigid wall," Rock and Soil Mechanics, vol. 42, no. 7, pp. 1839-1849, 2021.

[14] C. Y. Wang, X. P. Liu, Z. H. Cao, X. Jiang, and J. Q. Zhang, "Experimental study on characteristics of active slip surface of limited width soil behind rigid wall ," Rock and Soil Mechanics, vol. 42, no. 11, pp. 2943-2952, 2021.

[15] C. Y. Wang, X. P. Liu, Z. H. Cao, W. T. Mao, and Z. Z. Cai, "Experimental study on passive earth pressure and slip surface of limited width soil," Chinese Journal of Underground Space and Engineering, vol. 18, no. 4, pp 1250-1258, 2022.

[16] S. C. Wang, and H. Cheng, "Determination of active earth pressure behind retaining wall rotating about wall toe," Rock and Soil Mechanics, vol. 32, no. 7, pp 2139-2145, 2011.

[17] H. Z. Zhang, C. J. Xu, L. J. Liang, S. L Hou, R. D. Fan, and G. H. Feng, "Discrete element simulation and theoretical study of active earth pressure against rigid retaining walls under RB mode for finite soils," Rock and Soil Mechanics, vol. 42, no. 10, pp. 2895-2907, 2021.

[18] A. Arefnia, A. Dehghanbanadaki, and K. A. Kassim, "Sustainable implementation of recycled tire-derived aggregate as a lightweight backfill for retaining walls," KSCE Journal of Civil Engineering, vol. 25, no. 11, pp 4196-4206, 2021.

[19] H. A. Kamiloğlu, and E. Sadoğlu, "Experimental and theoretical investigation of short- and long-heel cases of cantilever retaining walls in active state," International Journal of Geomechanics, vol. 19, no. 5, pp 1-17, 2019.

[20] H. A. Kamiloğlu, and E. Sadoğlu, "Active earth thrust theory for horizontal granular backfill on a cantilever wall with a short heel," International Journal of Geomechanics, vol. 17, no. 8, pp 1-15, 2017.

[21] Y. Wang, H. B. Chen, G. P. Jiang, and F. Q. Chen, "Slip-line solution for the active earth pressure of narrow and layered backfills against inverted t-type retaining walls rotating about the base," International Journal of Geomechanics, vol. 23, no. 5, pp 1-14, 2023.

[22] Y. B. Zhang, F. Q. Chen, Y. J. Lin, and H. B. Chen, " Active earth pressure of narrow backfill against inverted t-type retaining walls rotating about the heel," KSCE Journal of Civil Engineering, vol. 26, no. 4, pp 1723-1739, 2022.

[23] E. Akis, "Optimum cost prediction of reinforced concrete cantilever retaining walls," Buildings, vol. 13, no. 10, pp 1-15, 2023.

[24] L. H. Zhao, S. Huang, Z. L. Zeng, R. Zhang, G. P. Tang, and S. Zuo, " Study on the ultimate bearing capacity of a strip footing influenced by an irregular underlying cavity in karst areas," Soils and Foundations, vol. 61, no. 2, pp 259–270, 2021.

[25] E. Cattoni, D. Salciarini, C. Tamagnini, " A Generalized Newmark Method for the assessment of permanent displacements of flexible retaining structures under seismic loading conditions," Soil Dynamics and Earthquake Engineering, vol. 117, no. 1, pp 221-233, 2019.

[26] Optum Computational Engineering Inc., 2019. Optum G2, Version 2019 User's manual, Denmark.

[27] GB50330-2013. Technical Code for Construction Slope Engineering. Standards Press of China, Beijing, 2013.

[28] A. J. Li, J. W. Mburu, C. W. Chen, and K. H. Yang, " Investigations of silty soil slopes under unsaturated conditions based on strength reduction finite element and limit analysis," KSCE Journal of Civil Engineering, vol. 26, no. 3, pp 1095-1110, 2022.

[29] J. X. Hua, and J. G. Zheng, Geological engineering handbook, 5th edition. Beijing, China: China Building Industry Press, 2018.

[30] Y. Que, X. F. Gui, and F. Q. Chen, "Active earth pressure against cantilever retaining walls with a long relief shelf in rotation about the top," KSCE Journal of Civil Engineering, vol. 27, no. 6, pp 2463-2476, 2023.

[31] K. A. Ranjbar, N. Ganjian, and F. Askari, "Stability analysis and design of cantilever retaining walls with regard to possible failure mechanisms: an upper bound limit analysis approach," Geotechnical and Geological Engineering, vol. 35, no. 1, pp 1079-1092, 2017.

[32] W. M. Yao, C. D. Li, C. B. Yan, and H. B. Zhan, " Slope reliability analysis through Bayesian sequential updating integrating limited data from multiple estimation methods," Landslides, vol. 19, no. 5, pp 1101-1117, 2022.

[33] W. C. Lv, A. G. Li, J. Y. Ma, H. H. Cui, X. Zhang, W. R. .Zhang, and Y. Z. Guo, " Relative importance of certain factors affecting the thermal environment in subway stations based on field and orthogonal experiments," Sustainable Cities and Society, vol. 56, no. 1, pp 1-10, 2020.

Dr. Yongqing Zeng was born in February 1991 and received his M.S.Degree from Anhui University of Science and Technology, Huainan, China, in 2016, and received the Ph.D. degree from Institute of Rock and Soil Mechanics, Chinese Academy of Sciences, Wuhan, China, in 2019. His research interests are mainly on geotechnical engineering. He is a lecturer in College of Civil Engineering and Architecture, Hunan Institute of Science and Technology, Yueyang, China. He authored or co-authored 25 journal papers and 5 international conference papers.

Jiawen Huang was born in September 1999 and received his B.E. degree from College of Civil Engineering, Xiamen University Tan Kah Kee College, Zhangzhou, China, in 2022. In the same year, he entered College of Civil Engineering and Architecture, Hunan Institute of Science and Technology, Yueyang, China for a master's degree. His research interests are mainly on geotechnical engineering.

Qisheng Hu was born in October 2005 and study in Civil Engineering at Department of Architecture and Civil Engineering, Hunan Urban Construction College, Xiangtan, China, in 2023. His research interests are mainly on geotechnical engineering.

Ruyi Zang was born in June 2004 and study in Nanhu College, Hunan Institute of Science and Technology, Yueyang, China, in 2022. Her research interests are mainly on geotechnical engineering.

Dr. Weidong Hu received the Ph.D. degree from Hunan Univesrtiy, Changsha, China, in 2016. Hu is the professor of College of Civil Engineering and Architecture, Hunan Institute of Science and Technology, Yueyang, China. His research interests cover excavation engineering and earth pressure. He has published more than 40 technical papers.

Dr. Xiaohong Liu received the Ph.D. degree from Central South Univesrtiy, Changsha, China, in 2011. She is the professor of College of Civil Engineering and Architecture, Hunan Institute of Science and Technology, Yueyang, China. Her research interests cover excavation engineering and earth pressure and non-contact testing of foundation deformation. She has published more than 30 technical papers.

Dr. Hua Luo was born in September 1985 and received her Ph.D. Degree from Beijing Jiaotong University, Beijing, China, in 2015. She is an associate professor in College of Civil Engineering and Architecture, Hunan Institute of Science and Technology, Yueyang, China. Her research interests cover bridge engineering and composite structure. She has published more than 20 technical papers.